Water Science & Technology

IWA PUBLISHING

Water Science & Technology Vol 88 No 11, 2986 doi: 10.2166/wst.2023.375

The utilization of microwaves in revitalizing peroxymonosulfate for tetracycline decomposition: optimization via response surface methodology

Tiehong Song[a], Yanjiao Gao [b,*], Hongyan Wei[a], Yu Zhao[a], Shujie Li[a] and Yi Jiang[c]

[a] Urban Construction College, Changchun University of Architecture and Civil Engineering, Changchun 130600, China
[b] College of Civil Engineering and Architecture, Liaoning University of Technology, Jinzhou 121001, China
[c] Key Lab of Songliao Aquatic Environment, Ministry of Education, Jilin Jianzhu University, Changchun 130118, China
*Corresponding author. E-mail: tmgyj@lnut.edu.cn; lngydxgyj@163.com

YG, 0000-0001-6915-855X

ABSTRACT

Antibiotic contamination in water has received significant attention in recent years for the reason that the residuals of antibiotics can promote the progression of antibiotic-resistant bacteria (ARB) and antibiotic-resistant genes (ARGs). It is difficult to treat antibiotics using conventional biological treatment methods. In order to investigate an efficient new method of treating antibiotics in water, in this study, microwave (MW) was employed in revitalizing peroxymonosulfate (PMS) to treat typical antibiotic tetracycline (TC). The Box–Behnken design (BBD) was applied to organize the experimental schemes. The response surface methodology (RSM) optimization was run to derive the best experimental conditions and validated using actual data. Moreover, the main mechanisms of PMS activation via MW were resolved. The results demonstrated that the relationship between TC removal rate and influencing factors was consistent with a quadratic model, where the *P*-value was less than 0.05, and the model was considered significant. The optimal condition resulting from the model optimization were power = 800 W, [PMS] = 0.4 mM, and pH = 6.0. Under such conditions, the actual removal of TC was 99.3%, very close to the predicted value of 99%. The quenching experiment confirmed that $SO_4^{\bullet-}$ and •OH were jointly responsible for TC removal.

Key words: Box–Behnken design, microwave, peroxymonosulfate, response surface methodology, tetracycline

HIGHLIGHTS

- MW/PMS was employed to treat tetracycline.
- BBD was applied to design the experimental protocol.
- The equation between TC removal and influences was established.
- RSM was used to predict optimal conditions.
- TC was co-oxidized by $SO_4^{\bullet-}$ and •OH to CO_2 and H_2O.

GRAPHICAL ABSTRACT

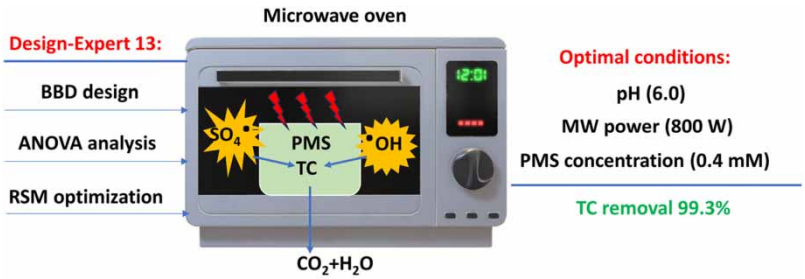

1. INTRODUCTION

Global production of pharmaceuticals in treating human and animal diseases is increasing, which results in more pharmaceuticals being released into the aquatic environment during their fabrication and utilization (Aus der Beek et al. 2016). Generally, the wastewater from pharmaceutical plants is pretreated and then sent to a municipal wastewater treatment plant for combined treatment with municipal wastewater. However, the predominantly biological processes in municipal wastewater plants are not efficient in eliminating pharmaceutical components from pharmaceutical plants, and some of the pharmaceuticals are still discharged into the receiving waters (Khasawneh & Palaniandy 2021). In addition, most of the pharmaceuticals used by humans and animals cannot be completely metabolized, and some of their residues also enter water bodies through excretion. Antibiotics are common pharmaceuticals that are widely employed to treat diseases caused by various bacteria. Antibiotic residue in the aquatic environment can promote the expansion of antibiotic-resistant bacteria (ARB) and antibiotic-resistant genes (ARGs) (Jovanovic *et al.* 2021). Since the chemical composition and structure of most antibiotics are complex, some conventional water treatment methods (coagulation, filtration, adsorption, biotreatment) cannot effectively remove them (Wang & Zhuan 2020). Therefore, efficient treatment methods for antibiotics in water should be continuously developed.

In recent years, the effects of advanced oxidation processes based on sulfate radicals ($SO_4^{\bullet-}$) have been affirmed in treating recalcitrant organics like antibiotics in water (Duan *et al.* 2020). Typically, two oxidizing agents persulfate (PS, $S_2O_8^{2-}$) and PMS (HSO_5^-) are applied in generating $SO_4^{\bullet-}$ under specific catalytic conditions (Honarmandrad *et al.* 2022). Since the redox potential of $SO_4^{\bullet-}$ ($E^0 = 2.5$–3.1 V) is higher than that of PS ($E^0 = 1.96$ V) and PMS ($E^0 = 1.75$ V), sulfate radicals are more capable of degrading organic pollutants (Chen *et al.* 2018; Scaria & Nidheesh 2022). A number of substances or energies can be employed in activating PS or PMS to yield $SO_4^{\bullet-}$, such as transition metals (Gao *et al.* 2018; Bouzayani *et al.* 2019), carbon materials (Kohantorabi *et al.* 2021; Gao *et al.* 2022), heat (Norzaee *et al.* 2018; Ahn *et al.* 2021), ultraviolet light (UV) (Alayande & Hong 2022), ultrasound (US) (Gujar *et al.* 2023), and microwave (MW) (Qi *et al.* 2014, 2017). The above methods are effective in removing recalcitrant organic pollutants from water. The principles for producing sulfate radicals via these methods are summarized in reactions as shown in Equations (1)–(6) (Wang & Wang 2018). The disadvantage of the transition metal activation is that excessive metal ions will be introduced into the water, bringing secondary pollution to the water. The carbon material activation has the problem of difficult recycling of carbon materials. Compared to these two methods, energy-based activation does not require materials or chemicals and is therefore an environmentally friendly approach.

$$S_2O_8^{2-} + M^{n+} \rightarrow SO_4^{\bullet-} + SO_4^{2-} + M^{(n+1)+} \text{ (M refers to transition metal.)} \quad (1)$$

$$HSO_5^- + M^{n+} \rightarrow SO_4^{\bullet-} + OH^- + M^{(n+1)+} \quad (2)$$

$$S_2O_8^{2-} + e^- \rightarrow SO_4^{\bullet-} + SO_4^{2-} \quad (3)$$

$$HSO_5^- + e^- \rightarrow SO_4^{\bullet-} + OH^- \quad (4)$$

$$S_2O_8^{2-} + MW(\text{heat, US, UV}) \rightarrow 2SO_4^{\bullet-} \quad (5)$$

$$HSO_5^- + MW(\text{heat, US, UV}) \rightarrow SO_4^{\bullet-} + HO^{\bullet} \quad (6)$$

Heat activation usually refers to the heating of the reaction solution with conventional heating methods (water bath heating, electric furnace heating) to obtain sufficient thermal energy. As the applied thermal energy is higher than the bonding energy of the O–O bonds of PMS or PS, the O–O bonds are broken and thus free radicals are produced. UV activation of PS or PMS is also an energy-based approach. UV is a form of light energy that is converted to heat when it hits the PMS(PS)/contaminant solution to be treated, thus activating the PMS or PS. But unlike heat activation, UV also excites some of the water molecules, generating hydroxyl radicals (Song *et al.* 2022). US applied to the reaction solution can generate localized higher pressure (500–5,000 bar) and temperature (1,000–15,000 K) in the aqueous solution through cavitation, which will cause PS or PMS activation to produce free radicals (Gujar *et al.* 2023). Similar to UV, the US can directly cavitate water to generate hydroxyl radicals. MW activation (frequency from 0.3 to 300 GHz) is preferred among several energy-based methods due to its ability to rapidly warm aqueous solutions and efficiently degrade organic matter. In addition to its use in water and waste treatment, MW has been explored in other fields as well, such as waste management and treatment, phase

separation and extraction processes, and remediation of soil (Bose & Kumar 2022; Shang *et al.* 2023). In this paper, we are more concerned with the application of MW in advanced oxidation methods for water treatment.

Some researchers have successfully degraded organic pollutants using MW-activated PS or PMS. For instance, MW/PS was employed to decompose sulfamethoxazole (Qi *et al.* 2014), methylene blue (KIm & Ahn 2014), pentachlorophenol (Qi *et al.* 2015), reactive Yellow 145 dye (Patil & Shukla 2015), humic acids (Zhang *et al.* 2018), imidacloprid (Genç & Durna 2018), sodium dodecyl benzene sulfonate (Bhandari & Gogate 2019), p-nitrophenol (Hu *et al.* 2019), dinitrodiazophenol (Wang *et al.* 2020), and tetracycline hydrochloride (Gao *et al.* 2020), and the influencing factors, kinetics, mechanism and acute toxicity were evaluated. MW has also been used as a coactivator for metal-activated PS, such as MW/zirconium oxide/PS degradation of methyl orange dye (Tantuvoy *et al.* 2023), and MW in assisting Cu-biochar to catalyze PS for the mineralization of oxytetracycline (Zhang *et al.* 2023). Furthermore, MW was applied to activate PMS in removing bisphenol A (Qi *et al.* 2017). MW was also used in combination with manganese ferrite to activate PMS for eliminating p-nitrophenol (Pang & Lei 2016). Feng & Li (2022) investigated the removal characteristics of NH_4^+–N and organic matter in the MW/PMS system with high Cl^- content, and found that $SO_4^{\bullet -}$, $HO^\bullet$ HOCl, and $Cl^\bullet$ played a major role in the removal of organic matter and NH_4^+–N in landfill leachate. Although MW/PS(PMS) processes have been reported in disposing of various recalcitrant organics, these processes have not been practically applied, thus more detailed studies are necessary. One aspect is that fewer studies of MW-activated PMS than activated PS have been reported, and no studies of tetracycline degradation by MW/PMS were found. Another aspect is that there is a lack of systematic optimization studies on the parameters of MW/PMS system in decomposing antibiotics.

In this study, MW/PMS process was applied to generate free radicals for typical antibiotic tetracycline (TC) decomposition. The entire data were analyzed using the software Design-Expert 13. The parameters of the experiment were set using Box–Behnken design (BBD) of the response surface methodology (RSM), the influencing factors were optimized depending on the resulting experimental data, and the dominant free radicals in MW/PMS system were also verified. Based on this study, the RSM method was used to optimize the reaction parameters of the MW/PMS system, which provided an effective method for predicting the removal rate of target pollutants.

2. MATERIALS AND METHODS

2.1. Chemical reagents

All chemical reagents used in this study were of analytical grade. TC and PMS (potassium monopersulfate triple salt) were purchased from Yuanye Biotechnology Co., Ltd (Shanghai, China). Tert-butyl alcohol (TBA) ($C_4H_{10}O$) was purchased from Maclean Biochemical Technology Co., Ltd (Shanghai, China), Methanol (CH_4O) was obtained from Kelong Chemical Reagent Factory (Chengdu, China), sodium hydroxide (NaOH) was obtained from Bohao Chemical Co. Ltd (Leping, China), and sulfuric acid (H_2SO_4) was obtained from Beijing Chemical Reagent Factory (Beijing, China). The aqueous solution to be treated was prepared by adding chemical reagents to deionized water.

2.2. Experimental

A MW apparatus (IEC 60335-2-90, Analytik Jena AG, Germany) was used for heating TC solutions. The ablation tanks containing premixed TC and PMS solutions were placed in the MW apparatus and the reactions were initiated by powering up the MW apparatus. The pH was regulated with 0.1 M H_2SO_4 or NaOH as needed. The MW power and reaction temperature were controlled by function keys on the MW apparatus. Samples were extracted every 10 min and 0.5 mL methanol was added to each sample bottle and filtered via a 0.22 μm filter membrane. The treated water samples were put into a UV-visible spectrophotometer (T-U9, Youke Instrument Co., Ltd, Shanghai, China) to detect the TC concentration at 357 nm.

To assess the effect of •OH and $SO_4^{\bullet -}$ on removing TC, two radical scavengers, methanol (MeOH), and TBA were employed in MW/PMS/TC process.

2.3. Box–Behnken design

The BBD was applied to the RSM design. The analysis and optimization of data were accomplished by software Design-Expert (version 13). RSM presents the quadratic model based on Equation (7) (Pelarti *et al.* 2022), where X_i refers to the coded independent variables; Y represents the dependent variable; i and j are index numbers; k is the number of patterns; β_0, β_i, β_{ii}, and β_{ij} are free term, linear, quadratic, and interaction effects, respectively; ε' is the random error between predicted

and observed values. The levels and independent variables are presented in Table 1.

$$Y = \beta_0 + \sum_{i=1}^{k} \beta_i X_i + \sum_{i=1}^{k} \sum_{j=1}^{k} \beta_i j X_i X_j + \sum_{i=1}^{k} \beta_{ii} X_i^2 + \varepsilon' \tag{7}$$

3. RESULTS AND DISCUSSION

3.1. BBD and analysis of variance

Design-Expert software (version 13) was employed to analyze the experimental data. According to the BBD (Table 2), 17 experiments were executed and the outcomes were optimized via quadratic equation as shown in Equation (8). Analysis of variance (ANOVA) is depicted in Table 3. The model *F*-value was 10.79 and *P*-value was 0.0024, implying it was significant. When *P*-value is less than 0.05, the model is considered significant. Moreover, the correlation coefficient $R^2 = 0.9328$, indicates that 93.28% variability can be resolved by this model.

$$\begin{aligned} TC(\%) = {} & 533.1 - 0.67675A - 622.875B - 33.1625C + 0.4225AB - \\ & 0.00425AC + 30BC + 0.000407A^2 + 280B^2 + 1.75C^2 \end{aligned} \tag{8}$$

Table 1 | The levels and independent variables

		Range and levels		
Independent variables	**Symbols**	**−1**	**0**	**+1**
Power (W)	A	600	700	800
PMS (mM)	B	0.2	0.3	0.4
pH	C	6	7	8

Table 2 | The coded and actual values based on BBD

				TC removal (%)	
Run	**A**	**B**	**C**	**Actual value**	**Predicted value**
1	700	0.3	7	82.3	81.9
2	800	0.3	6	89.3	89.9
3	700	0.3	7	81.5	81.9
4	700	0.4	8	91.1	91.9
5	800	0.2	7	78.3	78.5
6	600	0.4	7	90.8	90.6
7	700	0.3	7	81.4	81.9
8	700	0.2	6	87.8	87.0
9	600	0.2	7	90.5	88.8
10	700	0.3	7	80.4	81.9
11	700	0.2	8	73.5	75.7
12	700	0.3	7	83.9	81.9
13	700	0.4	6	93.4	92.2
14	800	0.4	7	95.5	97.2
15	800	0.3	8	86.2	83.7
16	600	0.3	6	88.4	90.9
17	600	0.3	8	87.0	86.4

Table 3 | ANOVA test for response function

Source	Sum of squares	DF	Mean square	*F*-value	*P*-value
Model	505.22	9	56.14	10.79	0.0024
A – Power	6.84	1	6.84	1.32	0.2890
B – PMS	207.06	1	207.06	39.82	0.0004
C – pH	55.65	1	55.65	10.70	0.0136
AB	71.40	1	71.40	13.73	0.0076
AC	0.7225	1	0.7225	0.1389	0.7204
BC	36.00	1	36.00	6.92	0.0339
A^2	69.92	1	69.92	13.44	0.0080
B^2	33.01	1	33.01	6.35	0.0398
C^2	12.89	1	12.89	2.48	0.1593
Residual	36.40	7	5.20		
Lack of fit	29.58	3	9.86	5.78	0.0615
Pure error	6.82	4	1.70		
Cor total	541.62	16			

The plot of normal probability of the externally studentized residuals is depicted in Figure 1. It is can be seen that the data points of the experiment were very close to a straight line, implying that the data belonged to the normal distribution and well suited to the quadratic model. Figure 2 exhibits the correlation between the predicted values and the actual values for TC removal. It was found that the actual values were very similar to the model predictions, indicating the validation and significance of predictive modeling of TC degradation (Eslami *et al.* 2016).

The RSM was applied to examine the interaction among the influencing factors on TC degradation efficiency, as shown in Figures 3–5. Figure 3 exhibits the interaction of PMS concentration and MW power towards TC removal, as pH remains constant. It can be seen from Figure 3, when the MW power increased from 600 to 800 W, TC removal rate rates showed an

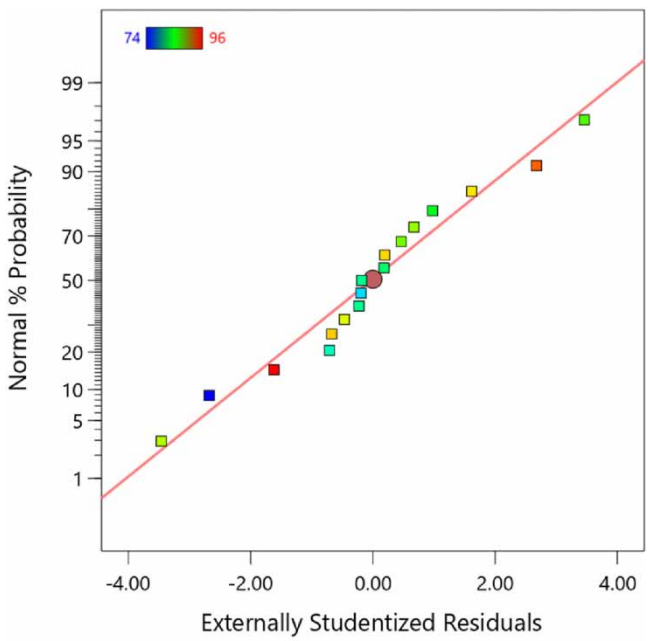

Figure 1 | Normal plot of the externally studentized residuals.

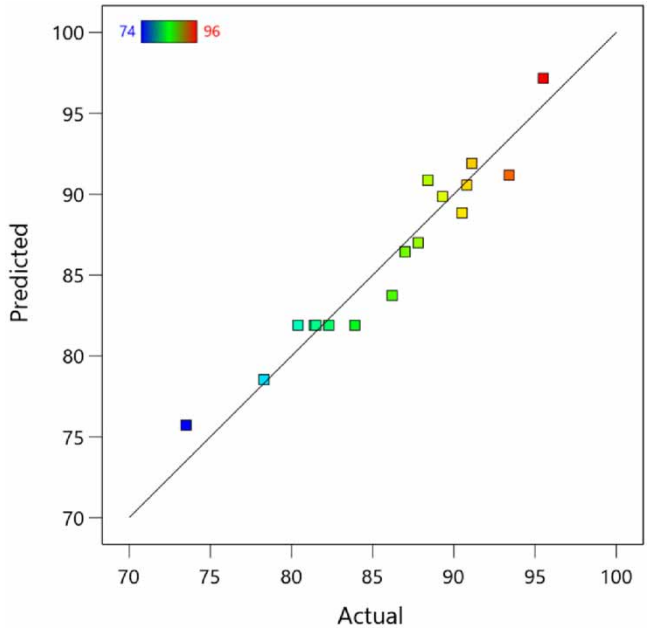

Figure 2 | Actual values versus predicted values for TC removal.

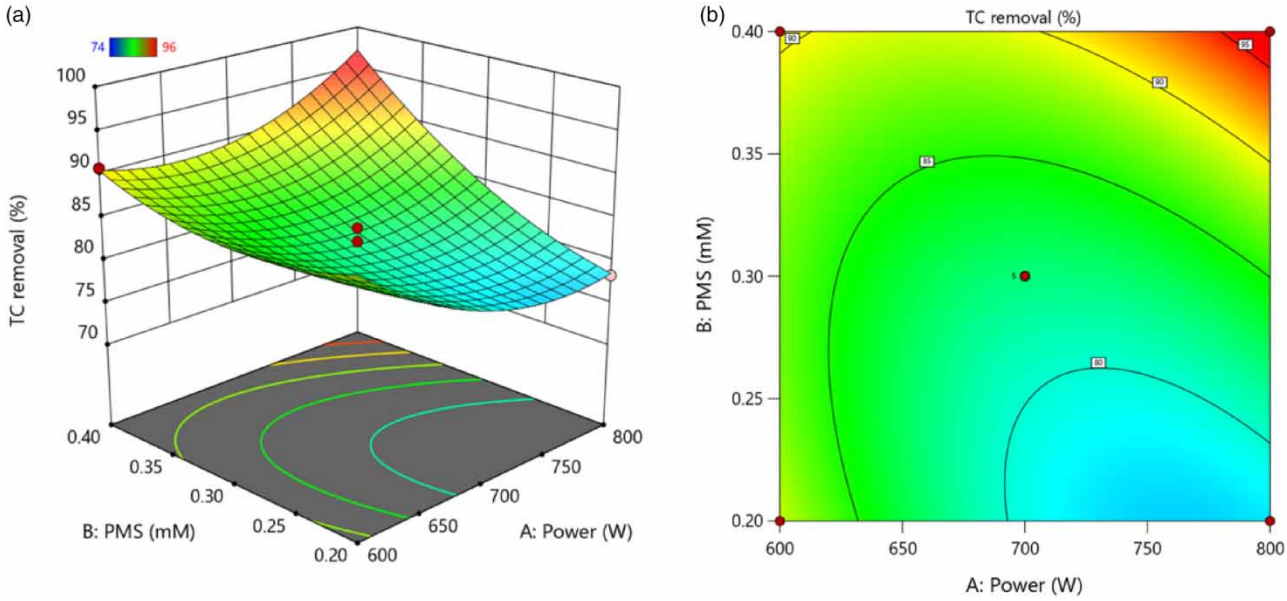

Figure 3 | The effect of PMS concentration and MW power on TC removal. (a) 3D; (b) 2D.

increasing trend. This is due to the fact that a high power helps the reaction solution to reach a high temperature for the same duration of time. The heat from the high temperature favors the O–O cleavage of PMS, which generates more free radicals (Equation (6)), and the high levels of free radicals in turn promotes TC decomposition. From Figure 4, it can be seen that as initial pH enhanced from 6.0 to 8.0, there was a slight decrease (about 9%) in TC removal. pH showed a significant impact on TC abatement in this system. As already mentioned, the activation of PMS by MW is based on its own high energy, which is not affected by pH. TC is an amphoteric chemical, and the overall charge of TC would present positive ($pH < 3.3$), neutral ($3.3 < pH < 7.7$), and negative ($pH > 7.7$) (Chao *et al.* 2017). The pH range for this experiment was 6–8, and the TC surface was essentially uncharged in this range, so the morphology of the TC itself had no effect on the degradation of the TC. However, PMS, as a precursor oxidant that produces free radicals, the difference in hydrolysis products (HSO_5^-, SO_5^{2-}) during the

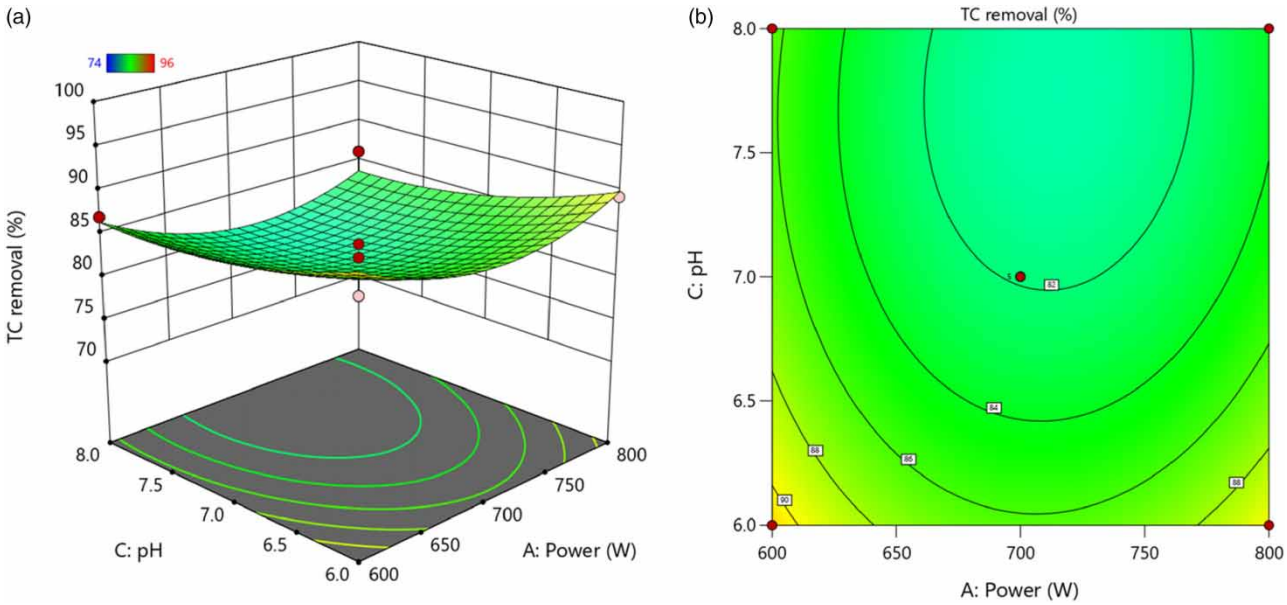

Figure 4 | The effect of pH and MW power on TC removal. (a) 3D; (b) 2D.

period at pH 6–8 will affect the amount of free radicals produced, which in turn will affect the treatment of the pollutants. This phenomenon was similar to the results of a previous study on the degradation of bisphenol A using the MW/PMS process in a pH range of 2.70–8.18 (Qi *et al.* 2017). Figure 5 exhibited the pH and PMS concentration on TC removal. It is found that PMS concentration played a significant role in TC degradation. With PMS concentration increased from 0.2 to 0.4 mM, the TC removal rate obviously kept increasing. PMS, as an oxidizing agent, is a source of •OH and $SO_4^{\bullet -}$, so an adequate supply of this agent promoted the formation of more free radicals, leading to more TC removed.

3.2. RSM optimization and validation

To optimize the parameters in MW/PMS system, a response optimizer was used. The highest TC removal (100%) was defined as the optimal target. The best values of independent variables (PS concentration, MW power, and pH) for TC degradation

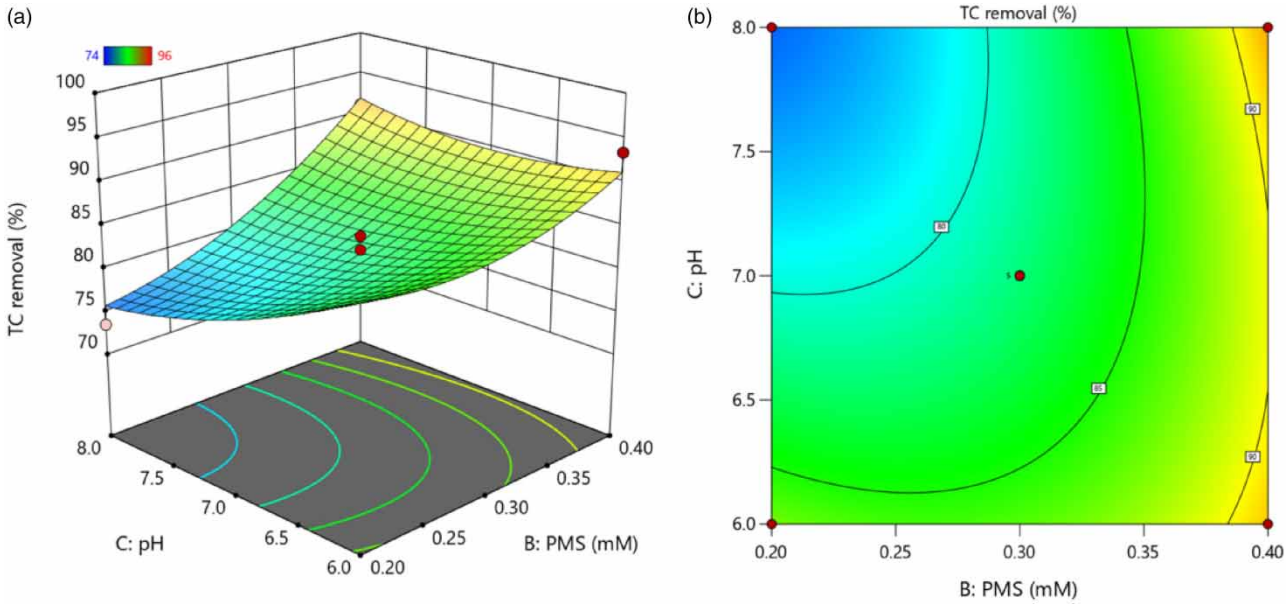

Figure 5 | The effect of pH and PMS concentration on TC removal. (a) 3D; (b) 2D.

are shown in Figure 6. To verify the reliability of the model, the experiment under the best-predicted conditions (power = 800 W, PMS = 0.4 mM, pH = 6.0) was carried out. The removal of TC of 99.3% was obtained, which was very close to the predicted TC removal of 99%. This indicates a very good match between the predicted and experimental values, which in turn confirms the reliability of the model.

3.3. Free radical quenching experiment

For the purpose of investigating which reactive species generated in MW/PMS system, quenchers MeOH and TBA were added in the system, respectively. MeOH has high rate constants for both $SO_4^{\bullet-}$ ($k = 1.0 \times 10^7\ M^{-1}{\cdot}s^{-1}$) and •OH ($k = 9.7 \times 10^8\ M^{-1}{\cdot}s^{-1}$), thus can quench both $SO_4^{\bullet-}$ and •OH. While TBA has a high rate constant for •OH ($k = (3.8–7.9) \times 10^8\ M^{-1}{\cdot}s^{-1}$) and a very low rate constant for $SO_4^{\bullet-}$ ($k = (4.0–9.1) \times 10^5\ M^{-1}{\cdot}s^{-1}$) and is therefore used to quench •OH only. The impact of quenchers towards TC elimination is depicted in Figure 7. Compared with the control curve, the removal

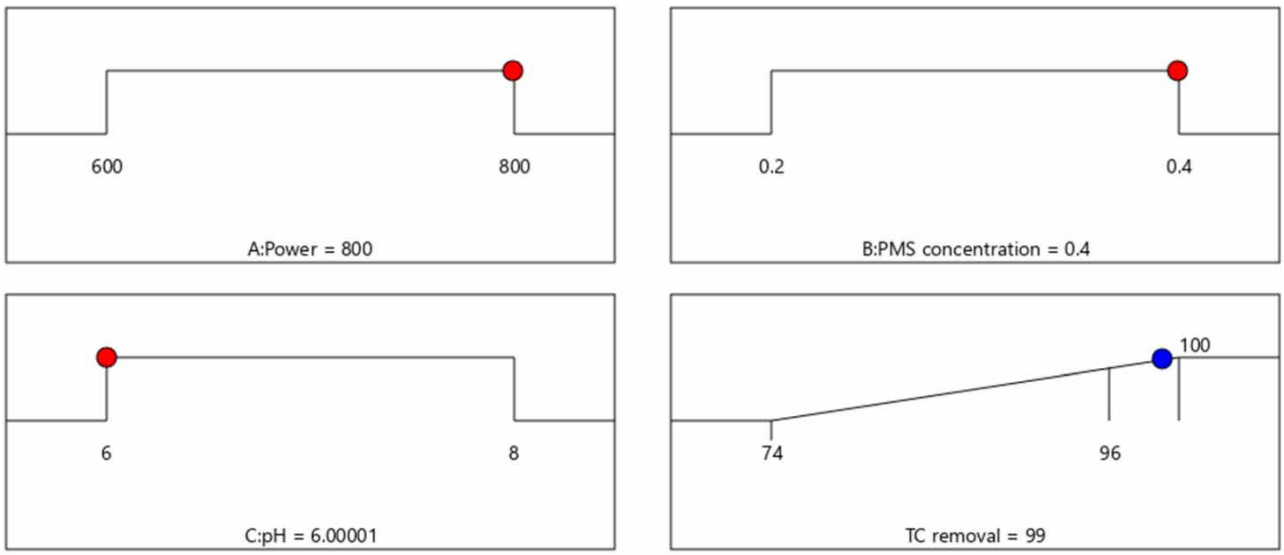

Figure 6 | Optimization of parameter values towards highest TC removal.

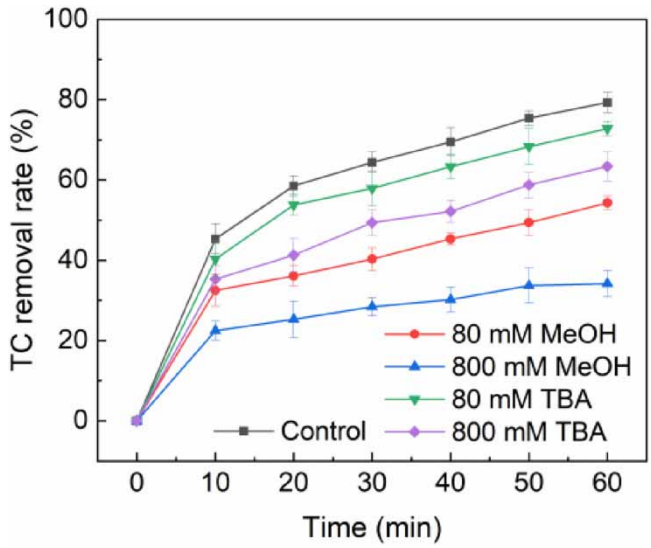

Figure 7 | The effect of MeOH and TBA. Conditions: [TC] = 20 mg/L, pH = 6.4, [PMS] = 0.2 mM, Power = 600 W.

of TC at 60 min by the MW/PMS system decreased from 79.3 to 72.8% and 63.4% when 80 mM TBA and 800 mM TBA were injected, respectively. This phenomenon demonstrates that •OH is formed during the reaction. When just the TBA was present in the MW/PMS/TC system, the TC removal dropped very quickly, from 79.3% at the control line to 34.2% at TBA of 800 mM and to 54.3% at TBA of 800 mM with 60 min of reaction. This confirmed that not only •OH but also $SO_4^{\bullet-}$ were generated in the MW/PMS/TC system. This result also coincided with the reaction mechanism of MW-activated PMS (Equation (6)).

4. CONCLUSION

In this study, the performance and mechanisms of MW/PMS system were demonstrated for the decomposition of TC. The RSM was utilized to model and analyze the impact of independent variables on TC removal. The quadratic model obtained had a high R^2 (0.9328), testifying that the model was reliable in predicting the experimental data. The optimum parameters predicted for TC removal (99%) were pH = 6, [PMS] = 0.4 mM, and MW powder of 800 W. The actual experimental result upon the optimal condition was very similar to the predicted result, proving that the developed model was very suitable for the MW/PMS system in this study. Also in terms of mechanism, it was concluded that $SO_4^{\bullet-}$ and •OH were produced in the MW/PMS process, which together acts on TC decomposition.

ACKNOWLEDGEMENTS

This work was supported by the Natural Science Foundation of Jilin Province of China, grant number YDZJ202201ZYTS681.

DATA AVAILABILITY STATEMENT

All relevant data are included in the paper or its Supplementary Information.

CONFLICT OF INTEREST

The authors declare there is no conflict.

REFERENCES

Ahn, Y. Y., Choi, J., Kim, M., Kim, M. S., Lee, D., Bang, W. H., Yun, E.-T., Lee, H., Lee, J.-H., Lee, C., Maeng, S. K., Hong, S. & Lee, J. 2021 Chloride-mediated enhancement in heat-induced activation of peroxymonosulfate: New reaction pathways for oxidizing radical production. *Environmental Science & Technology* **55**, 5382–5392.

Alayande, A. B. & Hong, S. 2022 Ultraviolet light-activated peroxymonosulfate (UV/PMS) system for humic acid mineralization: Effects of ionic matrix and feasible application in seawater reverse osmosis desalination. *Environmental Pollution* **307**, 119513.

Aus der Beek, T., Weber, F. A., Bergmann, A., Hickmann, S., Ebert, I., Hein, A. & Küster, A. 2016 Pharmaceuticals in the environment – global occurrences and perspectives. *Environmental Toxicology and Chemistry* **35**, 823–835.

Bhandari, P. S. & Gogate, P. R. 2019 Microwave assisted persulfate induced degradation of sodium dodecyl benzene sulfonate. *Korean Journal of Chemical Engineering* **36**, 2000–2007.

Bose, S. & Kumar, M. 2022 Microwave-assisted persulfate/peroxymonosulfate process for environmental remediation. *Current Opinion in Chemical Engineering* **36**, 100826.

Bouzayani, B., Rosales, E., Pazos, M., Elaoud, S. C. & Sanromán, M. A. 2019 Homogeneous and heterogeneous peroxymonosulfate activation by transition metals for the degradation of industrial leather dye. *Journal of Cleaner Production* **228**, 222–230.

Chao, Y., Yang, L., Ji, H., Zhu, W., Pang, J., Han, C. & Li, H. 2017 Graphene-analogue molybdenum disulfide for adsorptive removal of tetracycline from aqueous solution: Equilibrium, kinetic, and thermodynamic studies. *Environmental Progress & Sustainable Energy* **36**, 815–821.

Chen, J., Fang, C., Xia, W., Huang, T. & Huang, C. H. 2018 Selective transformation of β-lactam antibiotics by peroxymonosulfate: Reaction kinetics and nonradical mechanism. *Environmental Science & Technology* **52**, 1461–1470.

Duan, X., Yang, S., Wacławek, S., Fang, G., Xiao, R. & Dionysiou, D. D. 2020 Limitations and prospects of sulfate-radical based advanced oxidation processes. *Journal of Environmental Chemical Engineering* **8**, 103849.

Eslami, A., Asadi, A., Meserghani, M. & Bahrami, H. 2016 Optimization of sonochemical degradation of amoxicillin by sulfate radicals in aqueous solution using response surface methodology (RSM). *Journal of Molecular Liquids* **222**, 739–744.

Feng, K. & Li, Q. 2022 Chloride-enhanced removal of ammonia nitrogen and organic matter from landfill leachate by a microwave/peroxymonosulfate system. *Catalysts* **12**, 1078.

Gao, F., Li, Y. & Xiang, B. 2018 Degradation of bisphenol A through transition metals activating persulfate process. *Ecotoxicology and Environmental Safety* **158**, 239–247.
Gao, Y., Cong, S., He, Y., Zou, D., Liu, Y., Yao, B. & Sun, W. 2020 Study on the mechanism of degradation of tetracycline hydrochloride by microwave-activated sodium persulfate. *Water Science and Technology* **82**, 1961–1970.
Gao, Y., Wang, Q., Ji, G. & Li, A. 2022 Degradation of antibiotic pollutants by persulfate activated with various carbon materials. *Chemical Engineering Journal* **429**, 132387.
Genç, N. & Durna, E. 2018 Optimization of operational parameters by Taguchi design for imidacloprid oxidation by microwave-activated persulfate. *Environmental Progress & Sustainable Energy* **37**, 1632–1637.
Gujar, S. K., Divyapriya, G., Gogate, P. R. & Nidheesh, P. V. 2023 Environmental applications of ultrasound activated persulfate/peroxymonosulfate oxidation process in combination with other activating agents. *Critical Reviews in Environmental Science and Technology* **53**, 780–802.
Honarmandrad, Z., Sun, X., Wang, Z., Naushad, M. & Boczkaj, G. 2022 Activated persulfate and peroxymonosulfate based advanced oxidation processes (AOPs) for antibiotics degradation: A review. *Water Resources and Industry* **29**, 100194.
Hu, L., Zhang, G., Wang, Q., Wang, X. & Wang, P. 2019 Effect of microwave heating on persulfate activation for rapid degradation and mineralization of p-nitrophenol. *ACS Sustainable Chemistry & Engineering* **7**, 11662–11671.
Jovanovic, O., Amábile-Cuevas, C. F., Shang, C., Wang, C. & Ngai, K. W. 2021 What water professionals should know about antibiotics and antibiotic resistance: An overview. *ACS ES&T Water* **1**, 1334–1351.
Khasawneh, O. F. S. & Palaniandy, P. 2021 Occurrence and removal of pharmaceuticals in wastewater treatment plants. *Process Safety and Environmental Protection* **150**, 532–556.
Kim, Y. B. & Ahn, J. H. 2014 Microwave-assisted decolorization and decomposition of methylene blue with persulfate. *International Biodeterioration & Biodegradation* **95**, 208–211.
Kohantorabi, M., Moussavi, G. & Giannakis, S. 2021 A review of the innovations in metal-and carbon-based catalysts explored for heterogeneous peroxymonosulfate (PMS) activation, with focus on radical vs. non-radical degradation pathways of organic contaminants. *Chemical Engineering Journal* **411**, 127957.
Norzaee, S., Taghavi, M., Djahed, B. & Mostafapour, F. K. 2018 Degradation of Penicillin G by heat activated persulfate in aqueous solution. *Journal of Environmental Management* **215**, 316–323.
Pang, Y. & Lei, H. 2016 Degradation of p-nitrophenol through microwave-assisted heterogeneous activation of peroxymonosulfate by manganese ferrite. *Chemical Engineering Journal* **287**, 585–592.
Patil, N. N. & Shukla, S. R. 2015 Degradation of Reactive Yellow 145 dye by persulfate using microwave and conventional heating. *Journal of Water Process Engineering* **7**, 314–327.
Pelarti, M. M., Mirbagheri, S. A., Dehghan, K. & Alam, M. 2022 Nickel removal from aqueous solutions using flow-electrode capacitive deionization (Optimization by Response Surface Methodology (RSM)). *Water Science & Technology* **86**, 1299–1307.
Qi, C., Liu, X., Lin, C., Zhang, X., Ma, J., Tan, H. & Ye, W. 2014 Degradation of sulfamethoxazole by microwave-activated persulfate: Kinetics, mechanism and acute toxicity. *Chemical Engineering Journal* **249**, 6–14.
Qi, C., Liu, X., Zhao, W., Lin, C., Ma, J., Shi, W., Sun, Q. & Xiao, H. 2015 Degradation and dechlorination of pentachlorophenol by microwave-activated persulfate. *Environmental Science and Pollution Research* **22**, 4670–4679.
Qi, C., Liu, X., Lin, C., Zhang, H., Li, X. & Ma, J. 2017 Activation of peroxymonosulfate by microwave irradiation for degradation of organic contaminants. *Chemical Engineering Journal* **315**, 201–209.
Scaria, J. & Nidheesh, P. V. 2022 Comparison of hydroxyl-radical-based advanced oxidation processes with sulfate radical-based advanced oxidation processes. *Current Opinion in Chemical Engineering* **36**, 100830.
Shang, X., Liu, X., Ren, W., Huang, J., Zhou, Z., Lin, C., He, M. & Ouyang, W. 2023 Comparison of peroxodisulfate and peroxymonosulfate activated by microwave for degradation of chlorpyrifos in soil: Effects of microwaves, reaction mechanisms and degradation products. *Separation and Purification Technology* **306**, 122682.
Song, T., Li, G., Hu, R., Liu, Y., Liu, H. & Gao, Y. 2022 Degradation of antibiotics via UV-activated peroxodisulfate or peroxymonosulfate: A review. *Catalysts* **12**, 1025.
Tantuvoy, S., Kumar, M. & Nambi, I. 2023 Microwave assisted zirconium oxide based catalytic activation of persulfate for methyl orange dye degradation. *Journal of Environmental Chemical Engineering* **11**, 110721.
Wang, J. & Wang, S. 2018 Activation of persulfate (PS) and peroxymonosulfate (PMS) and application for the degradation of emerging contaminants. *Chemical Engineering Journal* **334**, 1502–1517.
Wang, J. & Zhuan, R. 2020 Degradation of antibiotics by advanced oxidation processes: An overview. *Science of the Total Environment* **701**, 135023.
Wang, Y., Guo, S., Gu, Z. & Zhang, A. 2020 Comparison study on microwave irradiation-activated persulfate and hydrogen peroxide systems in the treatment of dinitrodiazophenol industrial wastewater. *Chemosphere* **242**, 125139.
Zhang, X., Ding, Z., Yang, J., Cizmas, L., Lichtfouse, E. & Sharma, V. K. 2018 Efficient microwave degradation of humic acids in water using persulfate and activated carbon. *Environmental Chemistry Letters* **16**, 1069–1075.
Zhang, Q., Sun, Y., Xu, W., Cao, Y., Wu, C., Wang, C. H. & Tsang, D. C. 2023 Efficient microwave-assisted mineralization of oxytetracycline driven by persulfate and hypochlorite over Cu-biochar catalyst. *Bioresource Technology* **372**, 128698.

First received 23 August 2023; accepted in revised form 30 October 2023. Available online 18 November 2023